ASSESSMENT OF THE GALACTIC COSMIC RAY MODULATION FORECAST IN THE 25th SOLAR ACTIVITY CYCLE

© 2025 A.B. Struminsky [1,*], A.V. Belov [2], R.T. Gushchina [2], V.G. Yanke [2,], I.Yu. Grigoryeva [3]**

[1] Space Research Institute of the Russian Academy of Sciences (IKI RAS), Moscow, Russia

[2] Pushkov Institute of Terrestrial Magnetism, Ionosphere and Radio Wave Propagation of the Russian Academy of Sciences (IZMIRAN), Moscow, Troitsk, Russia

[2] Main (Pulkovo) Astronomical Observatory of the Russian Academy of Sciences (GAO RAS), Saint Petersburg, Russia

**e-mail: astrum@cosmos.ru*

***e-mail: yanke@izmiran.ru*

Received November 01, 2024

Revised December 11, 2024

Accepted December 12, 2024

The difference in the shape of galactic cosmic ray (GCR) flux maxima during positive ($A > 0$, minima of odd-even cycles) and negative ($A < 0$, minima of odd-even cycles) polarity of the Sun's dipole magnetic field is well known. During $A > 0$, a flat GCR maximum is observed, while during $A < 0$, a sharp one is observed. This difference is associated with the influence of the drift mechanism of GCR propagation in the global magnetic field of the heliosphere, *proxy* of which can be considered the polar (dipole) magnetic field of the Sun (B_{pole}). A homogeneous series of GCR data has been available since 1957, while observations of B_{pole} have been conducted only since 1976. Using the examples of odd (21st, 23rd, and 25th) and even (22nd and 24th) cycles, for which there are observations of B_{pole} and GCR, the hypothesis is investigated that changes in the magnitude and sign of B_{pole} determine the main trends in the development of the entire modulation cycle. Traditionally, the minimum of the sunspot number (R_z) is associated with the beginning of the 11-year cycle in long-term GCR modulation, but the growth of R_z does not reflect all physical processes on the Sun capable of modulating GCR in the heliosphere. We choose the beginning of the modulation cycle (zero on the time scale) as the maximum of GCR at 10 GV and then compare, using the epoch superposition method, the count rate of the Moscow neutron monitor, the values of B_{pole}, and R_z. With this choice of zero, the difference in the temporal profiles of GCR in even and odd cycles is clearly visible. When the modulus of B_{pole} decreases, GCR fluxes decrease, the convective transport mechanism predominates, and the drift transport effect is not visible (there is no explicit separation into even and odd cycles). When the modulus of B_{pole} increases, GCR fluxes increase, the diffusion mechanism of GCR transport predominates, which is either helped or hindered by the drift mechanism (at $A > 0$ or at $A < 0$). GCR fluxes remain constant when $B_{pole} \sim const$. Sunspot activity R_z is asymmetric relative to the moment of polarity reversal ($B_{pole} = 0$), it is early in even cycles and late in odd cycles. The identified trends allow us to qualitatively predict the corridor of possible changes in B_{pole} and GCR fluxes during the declining phase of cycle 25 and at the minimum of 25-26, as well as to make an epignosis based on observations of GCR and R_z of possible values of B_{pole} in 1957-76 (the end of the 19th and the entire 20th cycle).

Keywords: solar activity, even and odd cycles, polar magnetic field, heliospheric magnetic field, galactic cosmic rays, modulation

DOI: 10.31857/S00167940250303e4

1. INTRODUCTION

Galactic cosmic rays (GCRs) are highly energetic nuclei of fully ionized atoms that enter the heliosphere from the local interstellar medium (LIM). The energy spectrum of GCRs in the range from several tens of MeV to several GeV per nucleon is subject to modulation in the heliosphere depending on the phases of solar cycles. GCR intensities follow the 11-year solar activity (SA) cycle in anti-phase much better than any of the solar wind (SW) plasma characteristics measured at Earth's orbit: speed, density, and magnetic field. This is because the observed GCR intensity is the result of their interaction with the SW plasma in a large volume of the heliosphere. Therefore, GCRs can be considered as a "probe" for investigating the global properties of the heliosphere in various phases of the SA cycles. GCRs are also an ever-present source of radiation in interplanetary space (IP), whose characteristics must be taken into account when planning any activity in open space [Liu et al., 2024; Nymmik, 2007 and references therein].

The semi-empirical model of GCRs [Nymmik, 2007] takes into account experimental data on the particle flux at Earth's orbit depending on the level of solar activity, which is determined by the modulation function. The flux of the *i* -component of GCRs at Earth's orbit is the product of the empirical spectrum of the LIM-component in the LIM, which is defined by numerical coefficients, and the empirical modulation function. The value of the modulation function depends on the 12-month averaged sunspot numbers, the magnitude and direction of the large-scale heliospheric magnetic field, and the delay of modulation effects for particles with different rigidities. However, Nymmik's model [Nymmik, 2007] does not take into account experimental data on modulation in the weak 24th and current 25th SA cycles.

For many years, IZMIRAN has been developing a multiparameter semi-empirical model of long-period GCR variations. The model uses input parameters of cyclical changes in various solar indices (mean and polar magnetic field, inclination of the heliospheric current sheet, coronal mass ejection (CME) index, and area of equatorial coronal holes) and describes the behavior of GCR fairly well. Estimates of GCR variations in the 25th cycle using the forecast of solar indices are presented in the article [Yanke et al., 2024]. However, the solar activity indices used are the result of complex interaction between large-scale and local solar magnetic fields (see, for example, [Gushchina et al., 2008]). Solar activity indices may depend on each other, which allows for a reduction in the number of parameters with a physical, rather than statistical, approach to the GCR modulation problem. Possible schemes of interaction between magnetic fields of different spatial scales are presented in the works [Babcock, 1961 ; Owens et al., 2021] .

In the article [Yanke et al., 2024], it was noted that another approach is possible, "which suggests itself in the absence of the solar indices we need - to assume that the Sun in the 25th cycle will be similar to previous odd cycles." However, according to Yanke and co-authors Yanke et al. , 2024], such an assumption is unlikely to be correct. Despite this latter assertion, below we develop precisely this "other approach," in which the key point is the difference in GCR modulation in even and odd cycles, i.e., when the polarity of the solar dipole magnetic field (DMF) changes from $A < 0$ to $A > 0$ in even cycles and vice versa in odd cycles. Further observations of the 25th cycle will show which of the two approaches is better.

Obviously, with the "other approach," it is necessary to take into account the difference in GCR modulation effects in cycles with increased and decreased solar activity, in which the modulus of the DMF can differ by more than 3 times. *The proxy* for the DMF can be considered the polar magnetic field (PMF, B_{pole}) of the Sun; here by PMF we mean the results of standard observations and data processing conducted at the *Wilcox Solar Observatory* (WSO) since 1976 [Svaalgaard and Wilcox, 1978].

When discussing various methods of SA prediction, according to the review [Petrovay, 2020], methods using different precursors have outperformed extrapolation methods during the last few solar cycles, with polar magnetic field (PMF) observations being the best of all considered precursors. According to the authors of [Kumar et al., 2021], available observations and models indicate that the earliest time when PMF can be safely used as a precursor is 4 years after the reversal of the PMF sign, which usually occurs 2-3 years before the solar minimum and approximately 7 years before the predicted maximum. The possibilities of PMF epignosis for those time periods when its observations were not conducted or their data are not reliable were considered in [Wang, 2024]. In particular, it was shown that the observed values of radial IMF at the SA minimum can be used to reconstruct or refine PMF values and predict the SA cycle.

Unlike previous works by the IZMIRAN group on GCR modulation [Belov, 2000; Yanke et al., 2024 and references therein], here we will not use the results of variation calculations by the global survey method, but will limit ourselves to analyzing only the count rate of the Moscow neutron monitor (Moscow NM). This allows us to consider the latest current observations of the 25th cycle, however, it makes it impossible to study the energy spectrum of variations, which seems quite justified at the current stage of research. Moscow NM data are available from January 1958, while B_{pole} observations have only been conducted since May 1976. Therefore, in our study, we will consider GCR observations in cycles 19-25, and B_{pole} in cycles 21-25.

The beginning of the modulation cycle (zero on the time scale) is chosen as the maximum intensity of GCR with a rigidity of 10 GV, which was determined by the global survey method. Using the epoch superposition method, measurements of B_{pole} (http://wso.stanford.edu/Polar.html), monthly average sunspot numbers R_z (SSN Sun *Spot Numbers* https://www.sidc.be/SILSO/datafiles) and monthly average count rates of the Moscow NM (http://cr0.izmiran.ru/mosc/) in different SA cycles relative to the chosen zero are compared. This choice of zero corresponds to modern trends in understanding the physics of solar activity. According to estimates [Svaalgaard and Wilcox, 1978] polar fields are sufficient to explain most of the interplanetary magnetic flux. Traditionally, the minimum of sunspot number R_z is associated with the beginning of the 11-year cycle in the long-term modulation of GCR, but the growth of R_z does not reflect all the physical processes on the Sun capable of modulating GCR in the heliosphere [Cliver et al., 2013].

Analysis of methods and results of the 24th and 25th cycle forecasts [Nandy, 2021] showed that forecasts for the 24-25 cycles based on different methods diverged from each other, but only forecasts for the 25th solar cycle based on physical models converged, indicating a weak or moderately weak 25th sunspot cycle. According to Nandy [Nandy, 2021], such unity in predictions is a consequence of the available evidence that the Babcock-Leighton mechanism is the dominant driver of solar cycle variability on decadal time scales, and that the dynamic memory of the solar dynamo mechanism is short, allowing predictions only for the next sunspot cycle.

According to the review [Martin, 2024], a transition to a new paradigm of solar activity cycles is currently taking place. The old paradigm was based on observations of sunspots, and its further development was observations of magnetic fields in sunspot groups (active regions). In the old paradigm, solar cycles represented linear sequences of sunspot/active region cycles lasting about 11 years. For a complete magnetic cycle, two 11-year cycles were required. In the new paradigm, the emphasis has shifted from the 11-year sunspot cycle to the recognition of the extended solar cycle (see, for example, [Cliver, 2014]). In the extended solar cycle, besides spots, it is necessary separately to consider tiny (ephemeral) active regions that previously seemed insignificant. However, in total, they have a tremendous impact on the overall balance of magnetic fluxes in solar cycles. The beginning of each 22-year cycle coincides with the disappearance of the PMF of one polarity.

The aim of this work is to predict the possible modulation of GCR in the 25th cycle, based on the understanding of the dynamics of PMF and numbers R_z in even and odd cycles. Discussion of the possibility of epignosis of PMF in the 19th and 20th cycles of solar activity based on observations of R_z and variations of GCR. The basis for this will be the study of solar activity phenomena using the epoch superposition method relative to the selected time zero.

2. POLAR MAGNETIC FIELD OF THE SUN AND GCR MODULATION

2.1 Analysis of the transport equation

The distribution function of cosmic rays in the heliosphere *f* (**r** ; *t; R),* depending on time *t* , coordinates **r** and magnetic rigidity *R,* satisfies the transport equation [Parker, 1965; Gleeson and Axford, 1967; Fisk and Axford, 1969]:

$$\frac{\partial f}{\partial t} = -[\underbrace{\mathbf{V}}_{a} + \underbrace{\langle \mathbf{v_D} \rangle}_{b}] \cdot \nabla f + \underbrace{\nabla(\mathbf{k}_{(s)} \cdot \nabla f)}_{c} + \underbrace{\frac{1}{3}(\nabla \cdot \mathbf{V})\frac{\partial f}{\partial \ln R}}_{d}$$

The equation accounts for: (*a*) convection of CR by the solar wind (SW) with velocity *V* ; (*b*) drift of CR in the inhomogeneous heliospheric magnetic field (HMF) with effective drift velocity v_D(depends on *A* >0, *A* <0); (*c*) anisotropic diffusion on inhomogeneities of the interplanetary magnetic field (IMF), ($k_{(s)}$— symmetric part of the diffusion tensor); and (*d*) adiabatic energy losses caused by the dispersion of inhomogeneities. In this article, we do not discuss the energy spectrum of modulation, therefore we do not consider the term (*d*) in the transport equation. Here, by IMF we mean the characteristics of the magnetic field *in situ,* and by HMF — the integral characteristics of the global magnetic field throughout the entire volume of the heliosphere.

The number of CR particles *f(* **r** *; t; R)* increases due to (*c*), decreases due to (*a*). The authors of [Jokipi et al., 1977] were the first to understand that CR transport models in the SW should take into account drifts in the inhomogeneous magnetic field of the heliosphere. Drift effects in the HMF (*b*) can both increase the influx of particles into the inner heliosphere and decrease it depending on the field polarity and the sign of the particle charge. Drift effects can be considered as the introduction of an additional convection velocity v_D, which is added vectorially to *V velocity* of SW [Jokipi et al., 1977]. When *A* > 0, drift effects (*b*) will work against convective transport (*a*); i.e., they will supply protons to the inner heliosphere, and when *A* < 0, they will work against diffusion (*c*); i.e., they will transport protons out of the inner heliosphere.

Taking into account drift effects in the simplest HMF model, in which the current sheet separates Archimedean spiral magnetic fields of different directions, allowed explaining the shapes of two consecutive maxima of GCR intensity [Jokipii and Thomas, 1981]. Also, in this model, with a reasonable change in the tilt angle of the current sheet α from ~10 to ~30°, it was possible to obtain a change in GCR intensity comparable to that observed during the transition from minimum to maximum solar activity. At the same time, the authors of [Jokipii and Thomas, 1981] limited the applicability of their model to the period when α_t< 30°, since during periods closer to the SA maximum, one cannot expect a simple ordered structure of the HMF, as in the periods of SA minimum.

The success of the modulation model [Jokipii and Thomas, 1981] led to the establishment of the concept of the heliosphere as a sphere consisting of two unipolar "hemispheres" of opposite direction, separated by the heliospheric current sheet (see, for example, [Paouris et al., 2012; Stozhkov et al., 2022; Krainev et al., 2023]) for most of the SA cycle. According to [Krainev et al., 2023], the simple picture of a "two-hemisphere" heliosphere reflects the state of the LMF and is disrupted during periods of its polarity reversal—near the maximum of the SA cycle.

However, the interaction in the Sun's corona of magnetic fields of different spatial scales (global (poloidal) - of the order of the solar radius and local (torsional) - the size of an active region) can lead to the situation where the solar wind carries disordered magnetic field into the heliosphere not only when the main dipole field is minimal. According to the classical work [Babcock, 1961], it is the interaction of fields of different scales that leads to polarity reversal - the formation of a new main dipole field of reverse polarity. Since GCR modulation is sensitive to the polarity of the HMF (see Introduction section), it is possible to investigate the interaction of magnetic fields in the corona by studying the features of GCR modulation in even and odd cycles. The criterion for field interaction resulting in a chaotic HMF without a distinct polarity can be considered as the absence of influence of the sign of B_{pole} on GCR modulation.

2.2. Analysis of observational results

FIG. 1 .

The left panel of Fig. 1 shows the profiles of the monthly average count rate of Moscow neutron monitor in solar cycles 21-25, and the right panel shows the curves of the Sun's polar magnetic field strength obtained in solar cycles 21-25 according to Wilcox Observatory data through filtering and averaging (*filtered, average*). The left panel of Fig. 1 shows the separation of Moscow NM count rate profiles into two groups - even ($A > 0$) and odd ($A < 0$) solar cycles about ~5.5 years after the chosen zero. During the time interval (5.5-11) years, the Moscow NM count rate is higher in even cycles 22 and 24 than in odd cycles 21 and 23, which can be explained by the drift direction (b) in the HMF. From this, it can be concluded that in the four cycles considered, during the time interval (5.5-11) years, the HMF was not chaotic, and its predominant polarity was determined by the sign of the PMF (right panel of Fig. 1).

On the one hand, as expected, the NM count rate is higher in the weak 24th cycle than in the strong 22nd cycle, and this difference definitely exceeds local short-term variations. On the other hand, in the time interval (5.5-11) years in the pair of odd cycles 21st and 23rd, the difference in the NM count rate is comparable to the amplitude of local variations. Thus, in the time interval (5.5-11) years from the maximum of GCR, interactions of fields of different scales are not observed, i.e., the polarity of the solar dipole (polar field) predominates in the heliospheric field.

A different pattern of temporal profiles of the Moscow NM count rate is observed in the time interval (0-5.5) years, where there is no visible separation of NM count profiles into two groups of cycles - even and odd. This may be due to the fact that the HMF during the rising phase of solar cycles does not have a simple ordered structure characteristic of the solar dipole, as active generation of a new magnetic field of opposite polarity occurs during this time. As a result of this generation, the contribution of the DMF to the total magnetic field of the Sun gradually decreases, reaching zero near the maximum of the solar cycle - the moment of polarity reversal.

The slowest decrease in GCR intensity (Moscow NM) during the first three years after zero was observed in the weak 25th cycle with $A > 0$ (drift effects (*b*) "interfere" with convection (*a*) and "help" diffusion (*c*)), while the fastest decrease was in the strong 22nd cycle with $A < 0$ (drift effects (*b)* "help" convection (*a*) and "interfere" with diffusion (*c*). In the remaining three of the five cycles - 21st, 23rd, and 24th - rather large and overlapping variations are observed against the background of the general decrease in GCR intensity. Near the solar cycle maximum (the moment of the HMF polarity reversal), i.e., with minimal contribution of drift effects, the highest GCR intensity is observed in the weak 24th cycle, and the lowest in the strong 22nd cycle. In any case, for GCR intensity to decrease, it is necessary that in even cycles, the removal of particles from the heliosphere due to convection (*a*) and drift (*b*) be greater than their inflow due to diffusion (*c*); while in odd cycles, the removal of particles from the heliosphere due to convection (*a*) should be greater than their inflow due to drift (*b*) and diffusion (*c*).

FIG. 2.

The left panels of Fig. 2 show observations of odd SA cycles, and the right panels show even cycles. The upper panels present observations of the polar magnetic field. The curves B_{pole}

for odd cycles are compared with the dashed line - the curve B_{pole} for the 24th cycle, multiplied by (-1). It is evident that the polar field magnitude in odd cycles begins to change sharply later than in even cycles, (2.5-3.5) years relative to zero. In the odd 21st and 23rd cycles, the polar field magnitude does not stay near zero values for long and after ~5.5 years reaches a level close to (-50) mT. In the even 22nd and 24th cycles, the polar field magnitude stays near zero values longer (approximately for a year), but then quickly reaches and maintains its maximum values longer. Apparently, this is due to the fact that the generation of a positive polarity field is more efficient than a negative one . Negative (positive) magnetic helicity is observed predominantly in the Northern (Southern) solar hemispheres [Charbonneau, 2020].

The middle panels of Fig. 2 show the GCR modulation in odd (left) and even (right) cycles in grayscale. Predominant trends against the background of short-term variations are marked with straight lines. Until the moment of polarity reversal, GCR fluxes decrease with decreasing modulus of B_{pole} (according to the upper panels of Fig. 2), tracking the nature of its changes, and remain almost constant when B_{pole}~*const* (in particular, quasi-stationary states B_{pole}~ 0 near the GCR minimum). The GCR minimum phase, marked by horizontal straight lines in the middle panels of Fig. 2, occurs earlier in even cycles and lasts less than in odd cycles.

The lower panels of Fig. 2 show the curves of monthly mean sunspot numbers R_z in odd and even cycles. Straight lines show the general trends in R_z. Sunspot activity is asymmetric relative to the moment of B_{pole} (see upper panels), namely, it is "early" in even cycles and "late" in odd cycles.

Comparison of the right and left panels in Fig. 2 shows that odd cycles spend more time in the dynamic state of generating a field of new polarity and less time in the state of maximum polar field magnitude than even cycles. It is quite possible that such asymmetry of activity (visible in the polar field, GCR, and R_z numbers) qualitatively corresponds to the Gnevyshev-Ohl rule according to which the sum of spots in the preceding even cycle is less than in the subsequent odd cycle (see [Hathaway, 2015] and references therein). Indeed, in odd cycles, during the prolonged phases of maximum and declining activity, sunspots may appear (additional compared to the paired even cycle), necessary to fulfill the Gnevyshev-Ohl rule.

The discovered trends allow us to qualitatively predict the corridor of possible changes in B_{pole} and GCR fluxes during the declining phase of cycle 25 and in the minimum of cycles 25-26. It is also possible to try to reconstruct the assumed values of B_{pole} in 1957-76 (the end of the 19th and the entire 20th cycle) based on observations of R_z and GCR modulation.

3. FORECASTING OF THE 25th CYCLE AND EPIGNOSIS OF THE 19th AND 20th CYCLES

In order to understand possible GCR variations in the remaining years of the 25th cycle, it is necessary to understand the possible range of PMF changes. In Fig. 3 on the left, the light gray line of the polar field of the 25th cycle is continued by the upper envelope, according to the minimum values of PMF in the 23rd cycle and shows the upper limit of the "error corridor" values. The dashed line shows the PMF of the 24th cycle , taken with the opposite sign. The lower envelope goes down from the last measured value, taking into account the rate of negative PMF production in the 21st cycle up to its maximum magnitude.

FIG. 3.

When comparing the possible course of PMF of the 25th cycle (upper and lower envelopes) with the change in the polar field in the 21st and 23rd cycles, it can be seen that two bifurcation points may arise, approximately ~5.5 years and ~7.5 years after zero, which can sequentially lead to a strong polar field and a strong 26th cycle (like the 22nd) or to a weak polar field and a weak 26th cycle (like the 24th). According to the study [Jiang et al., 2015], the cause of the weak polar field and, consequently, the weak 24th cycle were large bipolar regions that appeared at low latitudes with the "wrong" (opposite to the majority) orientation in the north-south direction. The authors of [Kumar et al., 2024] managed to model the situation of polar field accumulation (see *fig* . 5D, in [Kumar et al., 2024]), reminiscent of the bifurcation point in the 21st and 23rd cycles, by changing the characteristics of bipolar regions. In the 25th cycle ($A < 0$), it will no longer be as weak as the 24th ($A > 0$) cycle, so the intensity of GCR in it will certainly be less than in the 24th. On the right panel of Fig. 3, the predicted range of changes in the count rate of the Moscow NM in the 25th cycle is highlighted by the upper and lower envelopes. We drew the upper envelope following the GCR intensity in the 19th cycle.

Note that the current monthly average number of sunspots has long exceeded the predicted maximum annual average SSN value of 127, which lies between the SSN maximums in the 20th and 24th cycles [Pal and Nandy, 2024]. Currently, the 25th cycle is close to the moment of the first bifurcation, and its unstable state is evidenced by sharp changes from 215.5 SSN in August to 141.4 SSN in September 2024. Let us document here our understanding of the further development of sunspot activity in the 25th cycle. In the case of development according to the scenario of the 23rd cycle, the activity maximum will occur in 1-2 years (2025-2026), with increased flare activity observed at lower R_z and less development of PMF. In the case of development according to the scenario of the 21st cycle, the maximum will occur in 2-3 years (2026-2027), and further, compared to the previous option, there will be more R_z and PMF development, but with minimal flare activity. Only passing through both bifurcation points will allow for more accurate estimates of the minimum of cycles 25-26 in 2030 and the further development of the 26th cycle.

In the paper [Jha and Upton, 2024], the statistical properties of active regions and characteristics of the 13th cycle, which is very similar to the current solar 25th cycle, were used to model advective transport of magnetic flux and forecast the evolution of PMF. According to the modeling results, the polarity reversal in the northern hemisphere of the Sun should occur b etween June and November 2024, with the center of distribution in August 2024. In the southern hemisphere, the polarity reversal should occur between November 2024 and July 2025, with the center in February 2025. Additionally, assuming that the axial dipole moment reversal coincides with the peak of the solar cycle, the maximum of the 25th cycle should have been between April and August 2024. Note that according to one of the authors (A. V. Belov), the maximum of the 25th cycle, at the time of submitting the article to the editorial office, most likely had already been passed.

Since the 20th sunspot cycle was stronger than the 24th but weaker than the 22nd, the maximum module of the polar field of the 19th cycle should be between the values of the weak and strong fields observed in the 23rd and 21st cycles, respectively. The end time of the polarity reversal in the 20th cycle can be determined by the beginning of the increase in GCR intensity, which was no later than the 7th year (i.e., earlier than in the 21st and 23rd cycles relative to zero). Modeling of the solar dipole moment [Pal and Nandy, 2024] showed that the 19th solar cycle is a notable exception among the cycles they considered. The calculated dipole moment differed significantly from the one estimated from observations, making it impossible to reconstruct the 20th cycle.

4. DISCUSSION. POLARITY OF THE HELIOSPHERIC MAGNETIC FIELD

The variations in the count rate of the Moscow NM in solar cycles 19-25 that we have considered, in our opinion, show the absence of visible influence of the HMF polarity during the time period (0, 5.5) years and its presence during the time period (5.5-11) years relative to zero. This conclusion is fully consistent with measurements of $2.0 \cdot 10^{8}$ electrons in the rigidity range from 1.00 to 41.9 GV over 11 years (2011-2022), presented by the *Anti Matter Spectrometer* (AMS) collaboration [Aguilar et al., 2023]. In this (so far the only) 11-year period, observations of electron fluxes show temporal variations clearly different from variations in proton fluxes. It should be noted that the variations in the AMS electron flux after 2016 correspond to the variations in the Moscow NM count rate in odd cycles 19th, 21st, and 23rd (Fig. 1 and Fig. 2). At the same time, there is no visible difference in the variations of electron and proton fluxes observed by AMS before 2016.

It follows that during the time periods (0, 5.5) years relative to zero in all the cycles considered, "chaotic" HMF prevailed without any pronounced polarity (field sign), and during the time periods (5.5-11) years, negative polarity prevailed in odd cycles and positive polarity in even cycles. Such behavior of the HMF corresponds to models of solar activity based on the Babcock-Leighton mechanism [Babcock, 1961; Leighton, 1964, 1969], which is regulated by the appearance of bipolar active regions inclined toward the equator and obeying the empirical laws of Hale and Joy (Hale et al., 1919).

The Babcock-Leighton mechanism (see review [Charbonneau, 2020]) consists of two processes: one is the annihilation of leading polarities in both hemispheres near the equator, the second is the drift and diffusion of the following polarity toward the pole. These unipolar magnetic regions neutralize the existing poloidal field at the pole and generate a poloidal field with opposite signs for the new solar cycle.

A qualitative scheme of interaction between global and local solar magnetic fields was proposed in the classic work Babcock, 1961], which suggests reconnection of magnetic field lines and, consequently, currents in the corona. In this scheme [Babcock, 1961], increasing field lines above the old bipolar magnetic region move upward and reach the field lines of the main dipole field. Gradually, breaks and reconnections occur so that part of the main field is neutralized. Also, a large loop with low-intensity flux is released in the corona. These weak flux loops are gradually released and begin to move upward with the coronal plasma, becoming the solar wind. In this case, the direction of the magnetic field frozen in the detached structure moving with the main solar wind flow is important.

During the growth phase of a new solar cycle, when it is necessary to neutralize the dipole field of the old cycle, the polarity of the magnetic field formed as a result of interaction and carried away with the solar wind turns out to be arbitrary. From the moment when the old dipole moment no longer exists, during the declining phase of the solar cycle, accumulation of a new dipole moment occurs, so the polarity of the large-scale field should coincide with the polarity of bipolar active regions. As a result, during the declining phase of the cycle, interactions between global and local fields do not occur, and the solar wind predominantly carries away field with the new polarity. The modulation of GCR convincingly demonstrates this.

In the review by Obridko [Obridko, 2008], certain features of existing methods for calculating global magnetic fields in the corona and interplanetary space are noted, which are based on the hypothesis of potential magnetic field on the photosphere surface. "The main limitation of the method is the forced assumption about the absence of currents in the Sun's atmosphere above the photosphere, which is inaccurate and even simply incorrect. Unfortunately, there are no other methods that allow relatively simple and quick calculation of the field in the corona." Models of the solar wind magnetic field calculated in the potential approximation are unlikely to correspond to observations.

The authors of the review [Khabarova et al., 2021] call on the scientific community to move away from the concept of the heliosphere as a 2D *D* freely expanding solar corona and non-interacting solar wind structures, which are described as flat or spherically symmetric objects. This picture has dominated for the past decades, but the need to account for the full diversity of the three-dimensional nature of heliospheric processes is becoming increasingly evident. The new 3D *D* approach provides an opportunity to understand the dynamics of heliospheric structures.

5. CONCLUSIONS

- Variations of cosmic rays observed in even and odd cycles indirectly confirm the chaotic mechanism of solar activity by Babcock-Leighton.
- Variations of GCR during the rising phase of a new solar cycle do not respond to the chaotic polarity of the HMF, but during the declining phase of the cycle, a clear

distinction in GCR variations between even and odd cycles is visible, corresponding to the polarity of the IMF after the reversal.

- The reversal is a lengthy process of changing the polarity of the IMF from the beginning of the decrease in the magnitude of the polar field in one of the hemispheres until the sign of polarity changes in both hemispheres of the Sun. The reversal of HMF lasts more than half a solar activity cycle, during this time GCR do not sense the polarity of the HMF. The HMF reversal is completed when the sign of the new solar polar field can be determined by GCR modulation; until this moment, the field of the old cycle is present in the heliosphere.
- A qualitative assessment of the corridor of possible changes in B_{pole} and GCR fluxes during the declining phase of the 25th cycle and in the minimum of the 25-26 cycles has been performed; possible uncertainties are associated with the chaotic development of the cycle in the Babcock-Leighton SA model. Considerations about possible values of B_{pole} in 1957-1976 (the end of the 19th and the entire 20th cycle) based on observations of R_z and GCR modulation are presented.

ACKNOWLEDGMENTS

The authors thank the observers and database creators (http://wso.stanford.edu/Polar.html and https://www.sidc.be/SILSO/datafiles) , whose work was used in this study, for their efforts and providing open access to the data. The authors are grateful to the teams of the World Network of CR stations and the NMDB project (https://www.nmdb.eu/).

FUNDING

The work was supported by subsidies for the themes "Plasma" at IKI RAS and "Multi-wavelength active Sun" at GAO RAS. The work at IZMIRAN was carried out within the framework of the UNU program "Russian National Ground Network of CR Stations".

REFERENCES

— *Gushchina R. T., Belov A. V., Obridko V. N., Shelting B. D.* Manifestations of cyclic variations of the Sun's magnetic field in long-term cosmic ray modulation // Geomagnetism and Aeronomy. Vol. 48. No. 5. pp. 598-604. 2008

— *Krainev M. B., Bazilevskaya G. A., Kalinin M. S., Mikhailov V. V., Svirzhevskaya A. K., Svirzhevsky N. S.* Fifty years of studying GCR intensity behavior during heliospheric magnetic field inversion periods. I. Observed effects //Solar-Terrestrial Physics. Vol. 9. No. 4. pp. 5-20. 2023

— *Nymmik R. A.* Model of galactic cosmic rays, Chapter 1.6 in the book Space Model: scientific information publication in 2 volumes. Edited by M. I. Panasyuk, L. S. Novikov. -Vol. 1: Physical conditions in space. Moscow: KDU, 2007. 872 p.: tables, illustrations.

— *Obridko V. N.* Magnetic fields and activity indices, paragraph 1.4 of Chapter 1 in the book Plasma Heliogeophysics. // In 2 volumes. Vol. I edited by L. M. Zelenyi and I. S. Veselovsky. Moscow: FIZMATLIT. 2008. - 672 p.

— *Aguilar M., Ali Cavasonza L., Ambrosi G., Arruda L., Attig N. et al., (AMS Collaboration)* . Temporal Structures in Electron Spectra and Charge Sign Effects in Galactic Cosmic Rays // Phys Rev Lett. V. 130. 161001. 2023. DOI: 10.1103/PhysRevLett.130.161001

— *Babcock H. W.* The topology of the Sun's magnetic field and the 22-year cycle //Astropys J. V. 133. P. 572–578. 1961. DOI: 10.1086/147060

— *Belov A.* Large scale modulation: view from the Earth // Space Sci Rev. V. 93. P. 79–105. 2000.
DOI: 10.1023/A:1026584109817

— *Charbonneau P.* Dynamo models of the solar cycle // Living Reviews in Solar Physics. V. 17. Iss. 4. 2020. DOI: 10.1007/s41116-020-00025-6

— *Cliver E.W.* The Extended Cycle of Solar Activity and the Sun's 22-Year Magnetic Cycle // Space Sci. Rev. V. 186. P. 169–189. 2014. DOI: 10.1007/s11214-014-0093-z

— *Cliver E.W., Richardson I.G., Ling A.G.* Solar Drivers of 11-yr and Long-Term Cosmic Ray Modulation // Space Sci. Rev. V. 176. P. 3–19. 2013. DOI: 10.1007/s11214-011-9746-3

— *Fisk L. A. and Axford W. I.* Solar Modulation of Galactic Cosmic Rays, 1 // J Geophys Res. V. 74. N 21. P. 4973-4986.1969. DOI: 10.1029/JA074i021p04973 .

— *Gleeson, L. J. and Axford, W. I.* Cosmic Rays in the Interplanetary Medium // Astrophys J. V. 149. P. L115–L118. 1967. DOI: 10.1086/180070
— *Hale G.E., Ellerman F., Nicholson S. B., Joy A. H.* The magnetic polarity of Sun-spot // Astrophys J. V. 49. P.153. 1919 . DOI: 10.1086/142452
— *Hathaway D. H.* The Solar Cycle // Living Rev Solar Phys. V. 12. P. 4. 2015. DOI: 10.1007/lrsp-2015-4
— *Jha B. K. and Upton L. A.* Predicting the Timing of the Solar Cycle 25 Polar Field Reversal // Astrophys J. V. 962. P. L15-L21. 2024. DOI: 10.3847/2041-8213/ad20d2
— *Jiang J., Cameron R. H., and Schüssler M.* The cause of the weak solar cycle 24 // Astrophys J Lett. V. 820. P. L28-L34. 2015. DOI: 10.1088/2041-8205/808/1/L28
— *Jokipii J. R, Levy E. H., and Hubbard W. B.* Effects of particle drift on cosmic-ray transport. I. General properties, application to solar modulation // Astrophys J. V. 213. P. 861−868. 1977. DOI: 10.1086/155218
— *Jokipii J. R., Thomas B.* Effects of drift on the transport of cosmic rays IV. Modulation by a wavy interplanetary current sheet // Astrophys J. V. 243. P. 1115−1122.1981. DOI: 10.1086/158675
— *Khabarova O., Malandraki O., Malova H., Kislov R.* et al. Current Sheets, Plasmoids and Flux Ropes in the Heliosphere Part I. 2-D or not 2-D? General and Observational Aspects // Space Sci Rev. V. 217:38. 2021. DOI: 10.1007/s11214-021-00814-x
— *Kumar P, Nagy M, Lemerle A, Karak B. B, Petrovay K.* The polar precursor method for solar cycle prediction: comparison of predictors and their temporal range// Astrophys J. V. 909. P 87−99. 2021. DOI: 10.3847/1538-4357/abdbb4
— *Kumar P., Karak B. B. and Sreedevi A.* Variabilities in the polar field and solar cycle due to irregular properties of bipolar magnetic regions // MNRAS. V. 530. P. 2895–2905. 2024. DOI: 10.1093/mnras/stae1052
— *Leighton R. B.* Transport of magnetic fields on the Sun // Astrophys J. V. 140. P. 1547–1562. 1964. DOI: 10.1086/148058
— *Leighton R. B.* A magneto-kinematic model of the solar cycle //Astrophys J. V. 156. P.1–26. 1969. DOI: 10.1086/149943

— Liu W., Guo J., Wang Yu., and Slaba T. C. A Comprehensive Comparison of Various Galactic Cosmic-Ray Models to the State-of the-art Particle and Radiation Measurements // Astrophys J. S. V. 271. P. 18−47. 2024. DOI: 10.3847/1538-4365/ad18ad
— *Martin S. F.* Observations key to understanding solar cycles: a review // Front. Astron. Space Sci. V. 10:1177097. 2024. DOI: 10.3389/fspas.2023.1177097
— *Nandy D.* Progress in Solar Cycle Predictions: Sunspot Cycles 24–25 in Perspective // Solar Phys. V. 296:54. 2021. DOI: 10.1007/s11207-021-01797-2
— *Owens M. J., Lockwood M., Barnard L. A. et al.* Extreme Space-Weather Events and the Solar Cycle // Solar Phys. V. 296:82. 2021. DOI: 10.1007/s11207-021-01831-3
— Pal S. and Nandy D. Algebraic quantification of the contribution of active regions to the Sun's dipole moment: applications to century-scale polar field estimates and solar cycle forecasting // MNRAS. V. 531. P. 1546–1553. 2024. DOI: 10.1093/mnras/stae1205
— *Parker E. N.* The Passage of Energetic Particles through Interplanetary Space //Planetary Space Sci. V. 13. P. 9–49. 1965. DOI: 10.1016/0032-0633(65)90131-5
— *Paouris E., Mavromichalaki H., Belov A, Gushchina R., Yanke V.* Galactic Cosmic Ray Modulation and the Last Solar Minimum // Solar Phys. 2012. V. 280. P. 255–271. DOI: 10.1007/s11207-012-0051-4
— *Petrovay K.* Solar cycle prediction. Living Rev Sol Phys. V. 17: 2. 2020. DOI: 10.1007/s41116-020-0022-z
— *Svaalgaard L. and Wilcox J.* A View of Solar Magnetic Fields, the Solar Corona and the Solar Wind in Three Dimensions // Ann Rev Astron Astrophys. V. 16. P. 429−443.1978. DOI: 10.1146/annurev.aa.16.090178.002241
— *Stozhkov Yu. I., Makhmutov V. S., Svirzhevsky N. S.* About cosmic ray modulation in the heliosphere // Universe. Vol. 8. Iss.11. P. 558. 2022. DOI: 10.3390/universe8110558
— *Wang Y.-M.* The Radial Interplanetary Field Strength at Sunspot Minimum as Polar Field Proxy and Solar Cycle Predictor //Astrophys. J Lett. V. 96. P. L27-L36. 2024. DOI: 10.3847/2041-8213/ad1c65
— *Yanke V. G., Belov A. V, Gushchina R. T., Kobelev P. G., and Trefilova L. A.* Forecast of Modulation of Cosmic Rays with Rigidity of 10 GV in the 25th Solar Activity Cycle // Geomagn Aeronomy. V. 64. N 2. P. 201–210. 2024. DOI: 10.1134/S0016793223601072

FIGURE CAPTIONS

Fig. 1. Moscow NM count rate (left panel) and the Sun's polar magnetic field (right panel) in solar activity cycles 21-25. On both panels, the open circle shows observations in September 2024.

Fig. 2. The magnitude of the polar magnetic field of the Sun (upper panel), monthly average count rates of NM Moscow (middle panel), and sunspot numbers (lower panel). The odd cycles of SA are shown on the left (on the middle and lower panels cycle 19 is added), and the even cycles are on the right (cycle 20 is added on the middle and lower panels). On the left panels, an open circle shows observations in September 2024.

Fig. 3. Forecast of the possible error corridor for the predicted values of the polar magnetic field (left panel) and NM Moscow count rate (right panel) for the remaining development period of cycle 25.

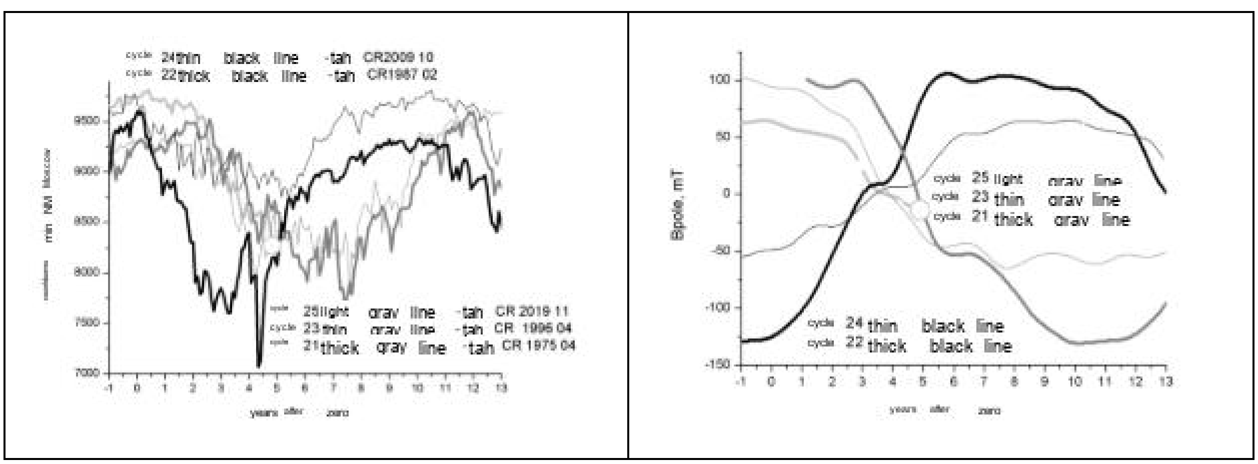

Fig. 1.

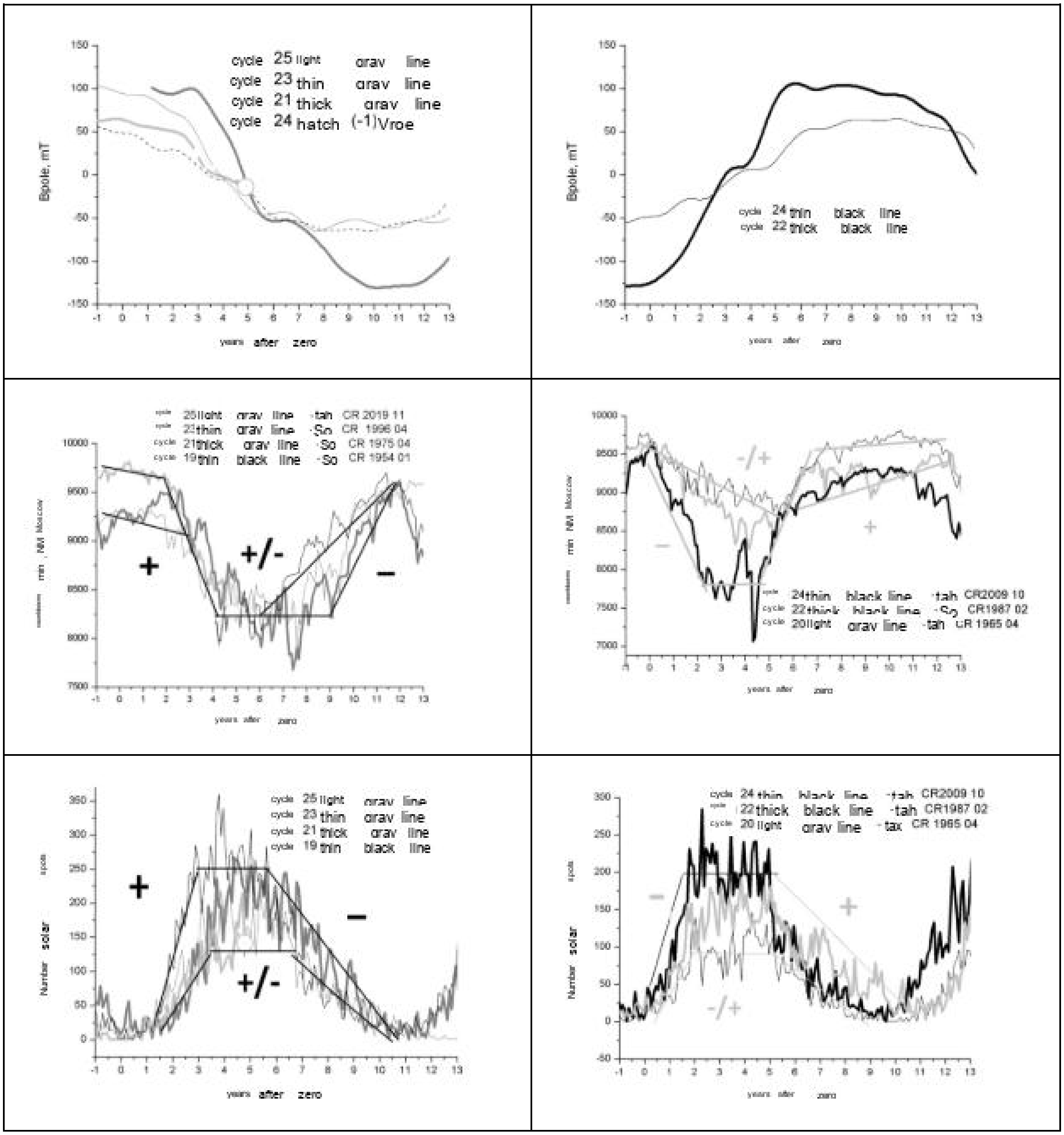
cycle 25 light grav line
cycle 23 thin grav line
cycle 21 thick grav line
cycle 24 hatch (-1)Vroe
Bpole, mT
years after zero
cycle 24 thin black line
cycle 22 thick black line
+
+/-
−
-/+
years after zero
solar Number

Fig. 2.

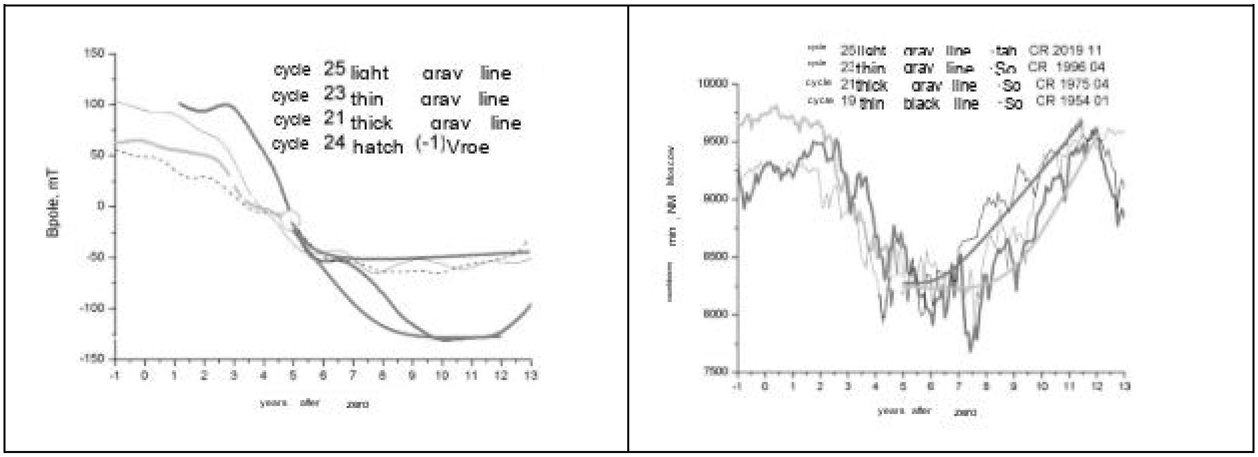
cycle 25 light gray line
cycle 23 thin gray line
cycle 21 thick gray line
cycle 24 hatch (-1)Vroe
Bpole, mT
years after zero
cycle 21 thick gray line -So CR 1975 04
cycle 19 thin black line -So CR 1954 01
years after zero

Fig. 3.